Impact of the assimilation of MSG/SEVIRI radiances in a mesoscale NWP model

by Thibaut Montmerle *
Météo-France/CNRM: 42, av. G. Coriolis 31057 Toulouse, France

Summary

The SEVIRI radiometer onboard MSG provides a complete set of radiance observations in the visible and the infrared spectrum every 15 min with an approximate spatial resolution of 5 km over Europe. Those measurements therefore seems to be particularly well adapted for the weather prediction at convective-scale, since they allow continuous access to information about the variation rates of temperature and humidity fields in space and time.
In order to quantify the impact of the assimilation of SEVIRI radiances in the analysis of those meteorological quantities, the regional NWP model ALADIN and its 3D-Var assimilation system have been used. SEVIRI data from the 12^{th} February 2003 case have been bias corrected, thinned and screened before the assimilation itself. Data from channels 3.9 μ and 9.7 μ have been blacklisted because of strong biases due to cloud contamination and/or calibration problem. Furthermore, a cloud detection scheme has been used in order to keep information above cloud top. The impact of the assimilation of the remained radiances leads to a reduction of the error in the humidity field in mid to high troposphere and to the humidification/drying of areas that allows a better prediction of mid to high level cloud cover. No impact have been observed in the analysis of the temperature field.

1 Introduction

The context of this work is the AROME project, which is Météo-France's future Numerical Weather Prediction (NWP) system at regional scale. This non-hydrostatic model, which is planned to run operationally around 2008, will cover the French territory with a 2.5 km horizontal resolution and will perform 1 to 2 hours data assimilation cycles using a 3D-Var algorithm. In this context of regional weather forecasting, the high horizontal and temporal resolutions of measurements performed by geostationary satellites are an asset compared to polar satellites, despite their weaker spectral and vertical resolutions. The purpose of this paper is to investigate the impact of the assimilation of SEVIRI IR observations in this context.
Since the AROME model still is in research phase, the study presented herein shows preliminary results of the assimilation of radiances observed by SEVIRI the 12^{th} of February 2003 in the 3D-Var assimilation system of the ALADIN model (Radnòti *et al.*, 1996). This spectral hydrostatic model, which is the LAM version of the global model ARPEGE/ IFS, covers the western Europe with a 10 km horizontal resolution. Its initial state and large scale conditions in the boundaries of its retrieval domain are given by ARPEGE outputs.

2 Experimental framework

ALADIN's 3D-Var can be used in research mode to assimilate the same types of observations than ARPEGE/IFS, that are among others radiosondes, ground station measurements, horizontal

*corresponding author's address: montmerle@cnrm.mete- o.fr

wind retrieved by geostationary satellites and radiances observed by the microwave radiometer AMSU-A onboard NOAA-16 and NOAA-17. The formalism of the variational analysis follows closely the work in ARPEGE/IFS (Courtier *et al.*, 1994).
To assimilate SEVIRI brightness temperature (T_b hereafter), this assimilation system has been modified in the following way: the analysis x^a represents the atmospheric state which is the best fit between the background x^b (usually taken as a 6 hour forecast) and the available observed radiances stored in the y vector. The cost function is written under an incremental formulation:

$$\begin{aligned} J(x) &= \tfrac{1}{2}\delta x^T \mathbf{B}^{-1}\delta x \\ &+\tfrac{1}{2}(\mathbf{H}\delta x - d)^T \mathbf{R}^{-1}(\mathbf{H}\delta x - d) \end{aligned}$$

Where δx is the increment defined by the difference between x^a and x^b; $\mathbf{B}$ is the background covariance error matrix computed using the "lagged NMC" method (Siroká *et al.*, 2002). This method is base on the computation of the$\mathbf{B}$ matrix from a pair of forecast valid at the same time, the short term run using the same lateral and initial conditions than the long term run. This allows to reduce the large scale variance and to get sharper analysis increments more adapted for mesoscale assimilation; $\mathbf{R}$ is the observation covariance error matrix; d the innovation vector that represents the departure between the observations and the background model state interpolated in the observation space:

$$d = y - H(x^b)$$

H being the observation operator that allows to write model variable in the observation space. The latter operator can be strongly non linear and contains i) the fast radiative transfer model RTTOV-6 (Saunders *et al.*, 1999), which allows to retrieve T_b from surface pressure and temperature and from vertical profiles of temperature, humidity and ozone, ii) a horizontal interpolation operator permitting to move the control variable profiles on observation locations, iii) a vertical interpolation and extrapolation operators allowing to position these profiles on RTTOV vertical levels. $\mathbf{H}$ is the tangent linear operator of H in the vicinity of the background state x^b. The variational problem is solved by calculating iteratively the cost function and its gradient:

$$\nabla_{\delta x} J = (\mathbf{B}^{-1} + \mathbf{H}^T\mathbf{R}^{-1}\mathbf{H})\delta x - \mathbf{H}^T\mathbf{R}^{-1}d$$

Convergence is obtained after $||\nabla_{\delta x} J||$ reaches a fixed minima.

3 Data preprocessing

The data used in this study comes from the 12^{th} February 2003, which corresponds to the first complete broadcasted SEVIRI image. At 13h30 UTC, these images are displaying a typical winter situation over western Europe characterized by an intense easterly moving low located south of Greenland, by an associated frontal rainband and by strongly anticyclonic conditions over eastern Europe that advects cold air westward, which produces stratus over Belgium and Germany.

3.1 Bias correction

The systematic error of the satellite data can be computed by looking at the innovation vector, as explained in (Harris and Kelly, 2001). This error arises mainly from errors in instrument calibration, radiative transfer model or from biases in model fields. To minimize the effect of the latter, only radiances near radiosondes are taking into account, since it is assumed that the model is relatively unbiased at these locations. Contrary to polar satellites, bias due to scan angles are negligible for geostationary platform, since these angles are small in this case.

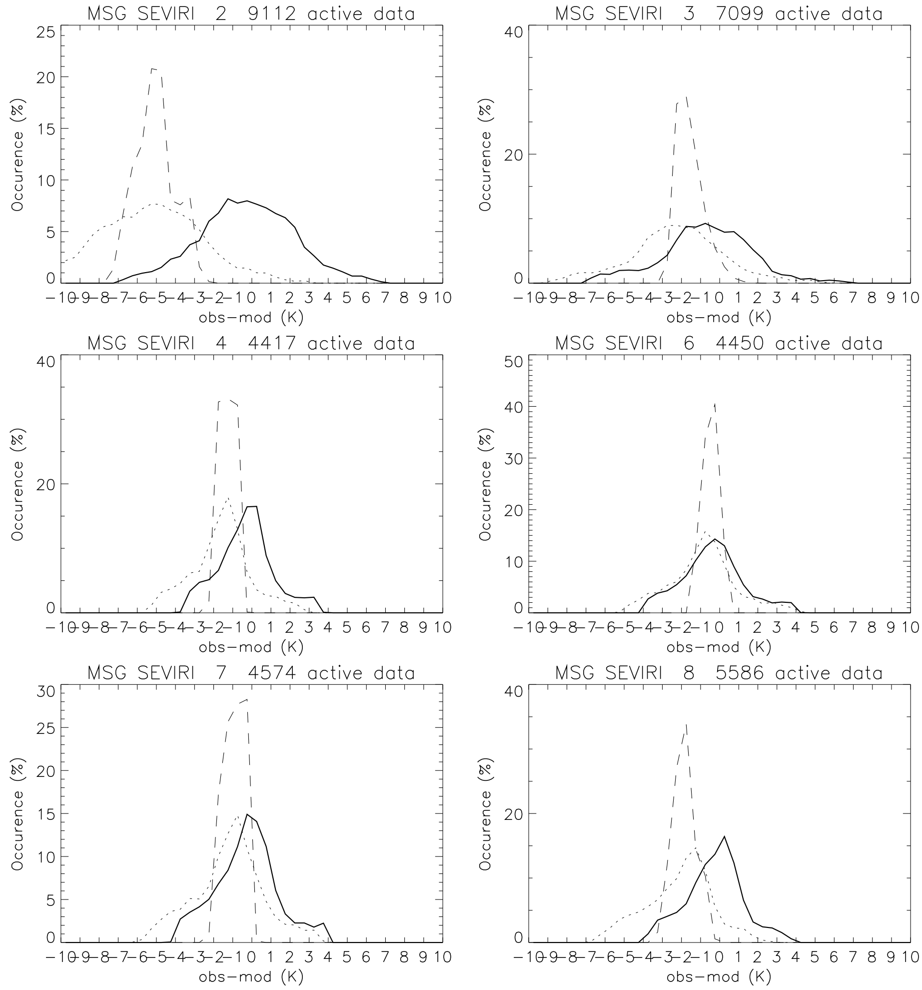

Figure 1: Histograms of T_b for the non-corrected background (dotted line), the applied bias correction (dashed line) and the corrected background (solid line) for the channels WV 6.2 μ (channel 2), WV 7.3 μ (3), IR 8.7 μ (4), IR 10.8 μ (6), IR 12.0 μ (7) and IR 13.4 μ (8)

The air-mass biases are computed for each channel using a multiple linear regression algorithm applied on four predictors that are 1000-300 hPa and 200-50 hPa thickness, model surface skin temperature and total precipitable water. The Fig. 1 shows the result of the bias computation for the six channels WV 6.2 μ, WV 7.3 μ, IR 8.7 μ, IR 10.8 μ, IR 12.0 μ and IR 13.4 μ. IR channels 3.9 μ and IR 9.7 μ have been blacklisted because of strong biases due to cloud contamination and/or calibration problem. For the resulting channels, some cases present strong initial bias (more than 5 K for WV 6.2 μ) which seems to confirm calibration problem for the studied situation. However, the innovation vector post-bias correction is well centered on zero, which indicates a good bias correction. To be really efficient, this method should be applied on several assimilation steps to take into account more data in the computation of the linear regression parameter and to perform monitoring. This point is part of the perspective of this work.

3.2 Screening

Once the bias correction has been completed, further successive operations on data are applied:

- **Cloud detection scheme:** the ECMWF clo- ud detection scheme devoted to the assimilation of AIRS radiances (Watts and McNally, 2002) has been adapted for SEVIRI radiances in order to detect channels that are non affected by cloud contamination. As a matter of fact, those channels are potentially useful by the assimilation system. This method allows to determine for each channel the level at which the presence of a single layer opaque cloud causes a 1 % change in the clear air radiance diagnosed from the model fields. For SEVIRI, it allows in most of cases to keep more data from the two WV channels since their weighting functions have a maximum above 600 hPa.

- **Quality control:** this check rejects data whose (obs-guess) value exceeds the sum of the background and the observation variances (σ_b and σ_o respectively) time an empirical constant α:

  $$((y - H(x^b))/\sigma_b)^2 \quad > \alpha(1 + \sigma_o^2/\sigma_b^2)$$

  The uncertainty of the humidity estimation in the troposphere leads to take a larger α for WV channels.

- **Thinning:** To keep the observations relatively uncorrelated, only one pixel over five has been taken into account in the process, which corresponds broadly to one observation every 30 km over Europe. Since the horizontal range of the analysis increment is around 100 km, this choice seems reasonable.

4 Impact of the assimilation of SEVIRI radiances

Results of the assimilation at 12 UTC of the observations out coming the screening process in ALADIN's 3D-Var is summarized on Fig. 2. This figure shows statistics on T_b for each SEVIRI channels separately. The distance between the two curves indicates how the addition of SEVIRI T_b could modify the background fields during the assimilation. A large reduction of RMS error can be seen for the two WV channels, which indicates that a large part of the information carried out by these channels have been taken into account in the analysis. Results are less notable for the 4 resulting IR channels, but their assimilation still is useful. For every channels, the bias are also smaller in the analysis. The cloud detection scheme leads to consider more WV observations (channels 2 and 3) and in a less obvious way T_b observed by the CO_2 absorption band channel (channel 8 at 13.4 μ).

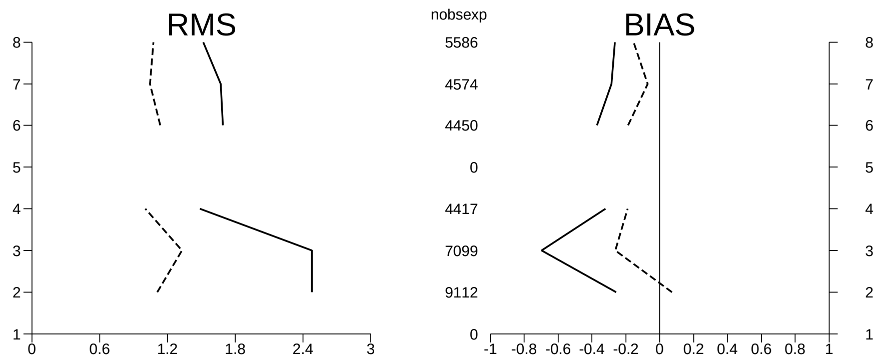

Figure 2: RMS error and bias for obs-guess (solid line) and obs-analysis (dashed line) after the assimilation of SEVIRI radiances. The ordinate axis represent the number of channel and the number of selected data after the screening

To quantify the impact of the assimilation of SEVIRI radiances on the analysis of temperature and humidity, comparisons have been undertaken between radiosondes measurements and values given by the background and the analysis interpolated at the launching sites. Fig. 3 displays such comparisons for 18 radiosondes performed in clear air conditions at the time of the assimilation over western Europe. A notable impact can be seen on the analysis of humidity in mid to high troposphere, with a 10 to 20 % error reduction compared to background values. On the other hand, the impact on temperature analysis is negligible. This can be due to the rather poor spectral resolution of SEVIRI channels, but also to the actual structure of the **B** matrix that leads sometimes to unrealistic information propagation along the vertical axis.

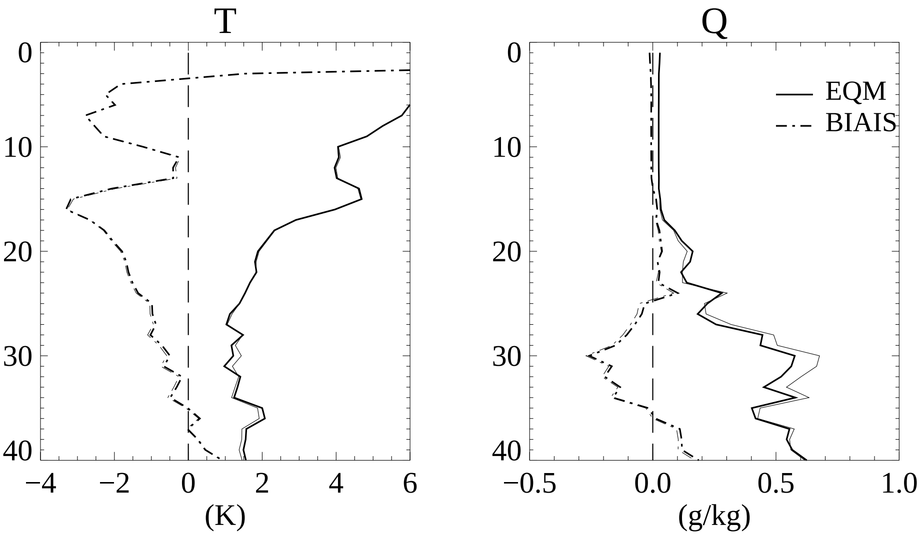

Figure 3: Mean standard deviation and bias profiles (solid end dashed lines respectively) of the difference between 18 radiosondes and the background (thin line) and the analysis (bold line) for the temperature (left column) and the humidity (right column)

5 Impact on short term forecast of cloud cover

During the previous sections, it has been shown that, after the assimilation of SEVIRI radiances (which corresponds to SEV experiment), the analysis increments generate humidification or drying of the mid to high troposphere in better agreement with in-situ measurements. The maximum values of those increments are from the same order of magnitude than those obtained after the assimilation of radiosondes (around 0.6 g/kg for the humidity field) (not shown). The impact on forecasts should therefore be seen on cloud cover fields, diagnosed from relative humidity and precipitations generated by the convection scheme. Comparisons of this quantities with NOAS experiment and Meteosat-7 images is displayed on Fig. 4 (NOAS corresponds to the prediction performed without any data assimilation).

In the SEV experiment, the most noticeable effect is that the atmosphere has been humidified upstream the frontal rain band and south east of Spain mostly around 750 hPa (not shown). After 24 hours forecast, this has permitted respectively to shift the frontal rain band eastward and to get a larger extent to the north of the large convective system located in south west Mediterranean see. The high level cloud cover is also more developed above the northern see. These features seem to be in better agreement with Meteosat WV image than NOAS.

6 Conclusion

SEVIRI data from the 12^{th} February 2003 case have been assimilated in the 3D-Var system of the regional LAM model ALADIN. These data have been firstly preprocessed: channel 3.9 and 9.7 μ have been blacklisted; a pixel-by-pixel air-mass dependent bias correction have been applied; a cloud detection sche- me has been adapted to take into account potential information above cloud top; a quality control check based on the examination of the innovation vector have been performed; data have been thinned. The impact of the assimilation of the resulting observations shows a reduction of the background error in mid to high troposphere for the humidity, mainly due to the information given by the two WV channels. No significant impact on the analysis of temperature has been noticed. The analysis increments lead to humidification or drying of certain areas with the same order of magnitude than increments obtained after radiosonde assimilation. 24 hours prediction shows mid and high level cloud cover in better agreement with observations.
To confirm those encouraging results, other cases have to be examined. Cycled assimilation with different frequencies (from 1 hour to 15 min) are currently under progress in order to study the potential contribution of SEVIRI's high temporal resolution vs. the high spectral resolution of AIRS-like radiometer. To maximize the impact of the assimilation of such observations at regional scale, some work has also to be done on the **B** matrix in order to take into account meteorological phenomena at that scale (such as low level inversion, position of a front...).

Acknowledgement: This work has been done thanks to a Alcatel Space financing.

References

Courtier, P., E. Andersson, W. Heckley, J. Pailleux, D. Vasiljevic, M. Hamrud, A. Hollingsworth, F. Rabier, and M. Fisher (1994). The ecmwf implementation of 3d-var. 1: Formulation. *Quart. J. Roy. Meteor. Soc. 120*, 1367–1387.

Harris, B. A. and G. Kelly (2001). A satellite radiance-bias correction scheme for data assimilation. *Quart. J. Roy. Meteor. Soc. 127*, 1453–1468.

Radnòti, G., R. Ajjaji, R. Bubnová, M. Caian, E. Cordoneanu, K. Von der Emde, J. Gril, J. Hoffman, A. Horányi, S. Issara, V. Ivanovici, M. Janoušek, A. Joly, P. Lemoigne, and S. Malardel (1996). The spectral limited area model ARPEGE-ALADIN. In *PWPRR Report*, Volume n.7, pp. 111–118. World Met. Org.

Saunders, R., M. Matricardi, and P. Brunel (1999). An improved fast radiative model for assimilation of satellite radiance observation. *Quart. J. Roy. Meteor. Soc. 125*, 1407–1425.

Siroká, M., C. Fisher, V. Cass, R. Brozkov, and J.-F. Geleyn (2002). The definition of mesoscale selective forecast error covariances for a limited area variational analysis. *Meteor. Atmos. Phys.*, 1–18.

Watts, P. and T. McNally (2002). A cloud detection approach for airs radiance assimilation. In *12th International TOVS study conference*, Australia.